

Experimental investigation on the seismic behavior of reinforced concrete column-steel beam subassemblies

Liquan Xiong^{1,2a}, Jinjie Men^{*1}, Ruyue Ren^{1b} and Mengke Lei^{1c}

¹ College of Civil Engineering, Xi'an University of Architecture & Technology,
13 Yanta Road, Xi'an, Shaanxi Province, 710055, China

² Department of Civil Engineering, Chongqing Three Gorges University,
666 Tianxing Road, Wanzhou, Chongqing Municipality, 404120, China

(Received March 13, 2018, Revised May 30, 2018, Accepted June 14, 2018)

Abstract. The composite reinforced concrete and steel (RCS) structural systems have larger structural lateral stiffness, higher inherent structural damping, and faster construction speed than either traditional reinforcement concrete or steel structures. In this paper, four RCS subassemblies with or without the RC slab designed following a strong column-weak beam philosophy were constructed and tested under reversed-cyclic loading. Parameters including the width of slab and composite effect of the RC slab and beam were explored. The test results showed that all specimens performed in a ductile manner with plastic hinges formed in the beam ends near the column faces. The seismic responses of composite connections are influenced significantly by different width of slabs. Compared with that of the steel beam without the RC slab, it was found that the load carrying capacity of composite connections with the RC slab increased by 30% on average, and strength degradation, energy dissipation also had better performance, while the ductility of that were almost the same. Furthermore, the contribution of connection deformation to the overall specimen displacement was analyzed and compared. It decreased approximately 10% due to the coupling effect in the columns and beams with the RC slab. Based on the test result, some suggestions are presented for the design of composite RCS joints.

Keywords: reinforced concrete column and steel beam; composite connections; slab; quasi-static test; seismic behavior; capacity; deformation

1. Introduction

The composite reinforced concrete and steel (RCS) structural systems that consist of reinforced concrete columns and steel beams have gained increasing interest in the past decades due to their efficiency from structural, economical and construction viewpoints compared with either traditional reinforced concrete (RC) or steel frames (Deierlein and Noguchi 2004, Li *et al.* 2011). On the one hand, using RC instead of steel columns can result in substantial savings in material cost and increase of inherent structural damping and lateral stiffness of the building, which lead to enhanced dynamic performance during lateral loading. On the other hand, steel beams take advantage of the long-span capabilities to provide column-free space and an efficient vertical spread of the construction activity.

Usually, this type of structural system has been used for low-to-mid-rise building construction in zones of low to moderate seismic risk (Viest *et al.* 1997). In such a system, the performance of joints had clearly different from that of

RC structure or steel structure. Many experimental programs were conducted by researchers for studying the behavior of the RCS joints (e.g., Moore and Gosain 1985, Wakabayashi 1985, Sheikh *et al.* 1989, Sakaguchi 1991, Parra-Montesinos and Wight 2000, Kuramoto and Nishiyama 2004, Gregoria and Harris 2012, Men *et al.* 2015, Alizadeh *et al.* 2015, Nie *et al.* 2017). The above test results have indicated that composite beam-column joints with reliable details which conventionally included the face-bearing plate, the embedded steel column, the band plate, and so on can provide very stable strength and ductile failure under reversed cyclic loading. Meantime, those results also showed basic mechanics provides understanding of the internal shear mechanisms and modes of failure that govern the RCS joint strength.

In addition, many researchers applied the finite element method to simulate the behavior of RCS beam-to-column connections. The nonlinear analysis of those specimens (e.g., Kim and Noguchi 1998, El-Tawil and Deierlein 2001, Cheng and Chen 2005, Shen 2007, Habashizadeh 2011) showed that (1) the model considering Interaction between the structural steel and concrete simulated the behavior of RCS frame specimens well; and (2) different factors influenced on performance of exterior composite RCS connections were discussed to provide theoretical foundation for design of composite RCS joints; and (3) Using of isotropic or kinematic hardening of steel materials at the finite element model may have a few effect on the

*Corresponding author, Professor,
E-mail: menjinjie@yahoo.com

^a Ph.D. Student, E-mail: xiongliquan2013@126.com

^b Master, Student, E-mail: 2811550846@qq.com

^c Master, Student, E-mail: 892706694@qq.com

behaviour of RCS connections under cyclic loading.

To learn more about the seismic performance of RCS connections about the composite effect of the RC slab and the steel beam. Some studies have been presented (e.g., Michael *et al.* 2000, Liang and Parra-Montesinos 2004, Cheng and Chen 2005, Bahman *et al.* 2012, Alizadeh *et al.* 2013, Nguyen *et al.* 2017). The results have indicated that the specimens performed in a ductile manner and showed a good strength and stiffness retention capacity.

The objective of the current research program is to evaluate composite effect of the RC slab and the steel beam for a novel RCS connection proposed by the authors (Men *et al.* 2015). Also the effect of different width of the RC slab on the mechanical behavior of the novel connections is discussed. The first section of the paper presents the specimen design philosophy and experimental program. In second section, the test results are detailed here in terms of cracking, yielding and failure mode, hysteretic behavior, strength degradation, energy dissipation capacity, and deformation. Finally, the effect of proposed detailing on the deformation performance of the RCS specimens was investigated.

2. Experimental program

In this investigation, four interior RCS subassemblies included three RCS beam-column-slab and one in-plane without the RC slab as a comparison model were constructed and tested under reversed-cyclic loading in Key Laboratory of Structural Engineering and Seismic Resistance, Ministry of Education, in Xi'an. A brief description of the design philosophy used for the test specimens, as well as their main features, is given in the following.

2.1 Design philosophy

The column-beam joint region mainly included details and strength was designed according to the ASCE design guidelines for composite connections (ASCE 1994); the composite beams were designed on the basis of the specification for structural steel buildings (AISC 2010); the RC columns and slabs were designed referring to the Chinese code for seismic design of buildings (CMC 2010a) and the ACI 318-14 (ACI 2014). In addition, a strong column-weak beam design philosophy was followed by designing the test specimens to have a column-beam moment strength ratio of approximately 1.4 for the three specimens, and approximately 1.6 for specimen #3 using

measured material properties and assuming full composite beam-slab behavior.

Two typically failure modes of the composite connections were identified as shear failure and bearing failure. It is desirable to design RCS joints to possess a good shear strength. Three components of the joint shear strength mechanisms concluded steel web panel, concrete compression strut, and concrete compression field. The behavior of the steel web panel acts similarly in composite and structural steel connections. The concrete compression strut activated through bearing of the concrete on the steel beam flanges and face bearing plates (FBPs) welded between the beam flanges at the column faces is similar to the mechanism used to model shear in reinforced concrete connections. The concrete compression field consists of several compression struts that act with horizontal reinforcement to form a truss mechanism outside the width of the steel beam flanges. In this experimental program, joint strength was checked according to the ASCE design guidelines for composite connections (ASCE 1994) and Parra-Montesinos and Wight (2001) to satisfy the target of a strong column-weak beam expected by researchers.

For the beam-through type of RCS connections, one of the main constructability problems in RCS systems is the detailing of transverse reinforcement in the beam-column joint region. In RCS frames, the ratio of steel to concrete volume at joint region is too high due to existence of continuous steel beams, joint stirrups, multiple details, and longitudinal reinforcement (reinforced concrete with an embedded steel shape for erection purposes). It causes some complication in construction and does not allow the concrete to fill the formwork properly. In terms of improving constructability, a novel detailing for RCS connections was proposed that the steel beam flanges extended to the joint were partly cut off, as shown in Fig. 1, which could keep the longitudinal reinforcement of the column passing through the connection. The detail concept

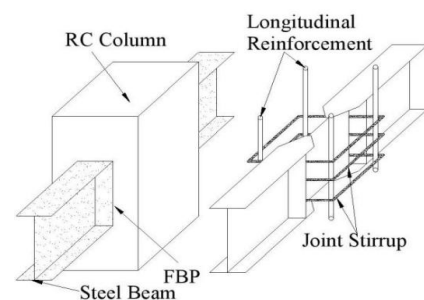


Fig. 1 Details of the novel RCS connection

Table 1 Features of specimens

Number	Details of joint	Moment strength ratio	Slab (mm)		Beam (mm)	Column		
			Thickness	Width		Measure	Stirrup	Reinforcement
Specimen #1	Face bearing plates /	1.4	60	845	HN 250×125 ×6×9	300×300 mm	8@50 /75 mm	12C16
Specimen #2	Cover plates /	1.4	60	1085				4C20+8C14
Specimen #3	Steel band plates /	1.6	60	1325				4C20+8C18
Specimen #4	Shear studs	1.4	0	0				4C16

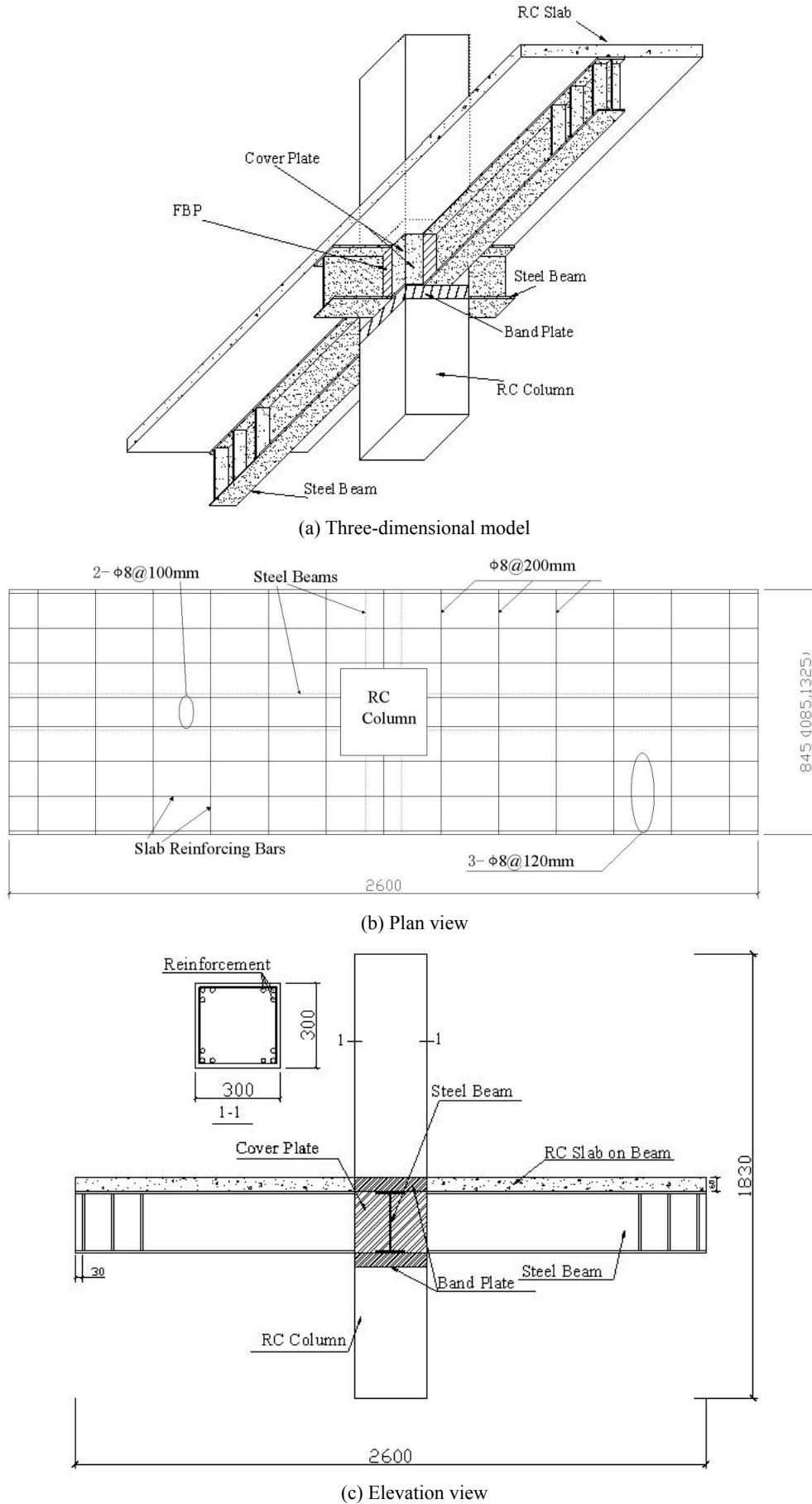


Fig. 2 Model of specimen

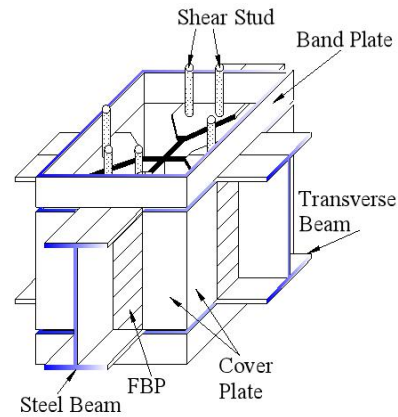
was also presented by Men *et al.* (2015) and Kuramoto and Nishiyama (2004)

2.2 Description of test specimens

The experimental program involved the testing of four approximately 1/2-scale beam-through type RCS specimens, and some features were described in Table 1. The overall specimen geometry and configuration are shown in Fig. 2. The specimens consisted of 2.6 m long structural steel beam that was framed in the continuous direction and the orthogonal beam coordinated with the width of slab in the discontinuous direction, upon which rested a rectangle RC slab (the length was 2.6 m, the width was a mainly variable parameter). Fig. 2(b) shows the RC slab reinforcing details for each of the specimens. These details have been varied to investigate the influence of the RC slab on the overall response. The structural steel beams consisted of HN 250×125×6×9 mm shape steel and were composed of Grade Q235 steel. The beams were framed into a 1.83 m high, RC column that was 300 mm square section. In one direction the steel beam was continuous through the RC column (hereafter referred to as the continuous direction). In the orthogonal direction (discontinuous direction) the beams were connected to the joint using various detailing arrangements, further details of which will be given later. All welds used E45XX electrodes and were sized to develop the full strength of the connecting element.

The thickness of the RC slab placed on top of the steel beams, with the ribs mainly parallel to the main beam, was 60 mm for all the test specimens. Composite action between the RC slab and the steel beam was enforced by stick welding 14 mm diameter, 45 mm long headed shear studs to the top flange of the steel beams embedded the RC slab. Twenty four studs were used on continuous beam between the column and edge of slab with the double lines, spaced an average of 100 mm on center, with the first stud 20 mm away from the face of the column. while studs were chosen in a single line with the same geometry in the discontinuous direction in coordination with the RC slab. The number of shear studs was welded to the top beam flanges to achieve full composite behavior between the steel beam and RC column in RCS joints. The RC slab was reinforced with 8 mm diameter reinforcing bars spaced an average distance of 120 mm apart in the continuous direction and that of 200 mm in the discontinuous direction (Fig. 1) on the top layer, respectively, and the same form of that on the bottom layer. The amount of reinforcement placed in the RC slab was chosen as that required for full composite action. This amount of reinforcement was included to increase the stiffness of the composite beam section and negative bending strength that allowed any developed reinforcement within the effective slab width to make contribution.

The type of composite connection details for the specimens, shown in Fig. 3, was used in the experimental program consisted of face bearing plate (FBP), shear stud, band plate, cover plate and transverse beam. The details of connection were made in accordance to current the RCS connection design guidelines (ASCE 1994) and the study by Men *et al.* (2015). The first character, FBP, was 230×60×8



(a) Design



(b) Production

Fig. 3 Proposed specimen details

mm and was fillet welded to all beams at the beam-connection interface to mobilize the shear resistance of the inner diagonal concrete strut in the RCS joint region. To prevent bearing failure of the column concrete that faces the steel beam, the second character, Grade 4.6 shear stud, with a length of 100 mm and a diameter of 22 mm was welded to the beam flanges provided a means of transferring force from the flange to the concrete as recommended by Sheikh *et al.* (1989). The third character utilized connection detailing that consisted of band plate to form a square connection region with the same dimensions as the column. In addition, band plates were fillet welded above and below the beam flanges with a height of 60 mm and a thickness of 8 mm to strengthen the joint region against vertical bearing failure by providing confinement to the concrete in the critical bearing zones. The fourth character, steel cover plates, with a thickness of 8 mm were welded to the FBPs and beam flanges by means of full penetration welding to form a square joint region surrounded the column armed to replace the stirrup in the RCS joint for construction simplicity. Additionally, the previously mentioned studies clearly showed the behavior of the steel cover plates was an effective measure to confine the concrete inside it developed by Men *et al.* (2015). The transverse beams that were framed in the discontinuous direction were connected to the joint with the details given former to enhance discontinuous beam strength and stiffness.

Specimen #1 was designed to study the seismic performance of the specimen with the RC slab which was a

width of 845 mm (Table 1 and Fig. 2). Column longitudinal reinforcement included twelve C16 mm deformed bars representing approximately 2.68% of the column gross area. A8 bars were used for column stirrups. Three layers of closed rectangular stirrups spaced an average distance of 50 mm were provided in the column region immediately above and below the band plates, while the rest of stirrups with the distance of 75 mm were designed. The band plates in specimen #1 replaced the column stirrups required and allowed the elimination of joint transverse reinforcement, enabling transverse beams to frame into the main beam at the connection region as recommended by Liang and Parra-Montesinos (2004).

Specimens #2 and #3 were designed to learn more about the performance of the specimens with the different width of slabs. The configuration and details of specimens had the same design as specimen #1, respectively, except that the width of slabs were 1085 mm and 1325 mm to consider the inelastic connection response corresponding to increase the amount of reinforcement (Table 1 and Fig. 2). Column longitudinal reinforcement for specimen #2 included four C20 mm and eight C14 mm, and that of specimen #3 included four C20 mm and eight C18 mm, respectively. Specimen #4 was designed to extend the work performed by researchers studying the in-plane connection behavior of RCS systems as a comparison model for the other specimens. Specimen #4 had the same design as specimen #1 without the RC slab and orthogonal beam, except that column longitudinal reinforcement included four C16 mm deformed bars.

2.3 Material properties

To ensure the consistency of the specimens, concrete in all specimens was poured and strictly compacted in a certain period. The concrete compressive strengths f'_c for columns and slabs at test day were 25.13 MPa, which was obtained based on three cubes for each concrete pour. All the steel components were fabricated in the factory. Grade HRB400 deformed steel bars were used for all the reinforcement in the columns, exclude 8 mm diameter rebars which were Grade HRB300. The material properties from the tensile tests for each of the steel plates and rebars are listed in Table 2.

Table 2 Material test of the steel plates and rebars

Material type	f_y (MPa)	f_u (MPa)	E_s (10^5 MPa)
Beam flange	265.0	406.7	2.10
Beam web	231.7	380.0	2.00
Face bearing plates/ Cover plates/ Steel band plates	278.3	398.0	2.01
A8 bars	448.3	496.7	2.09
C14 bars	436.7	597.7	2.04
C16 bars	438.3	600.0	1.98
C18 bars	433.3	588.3	2.02
C20 bars	416.7	596.7	2.02

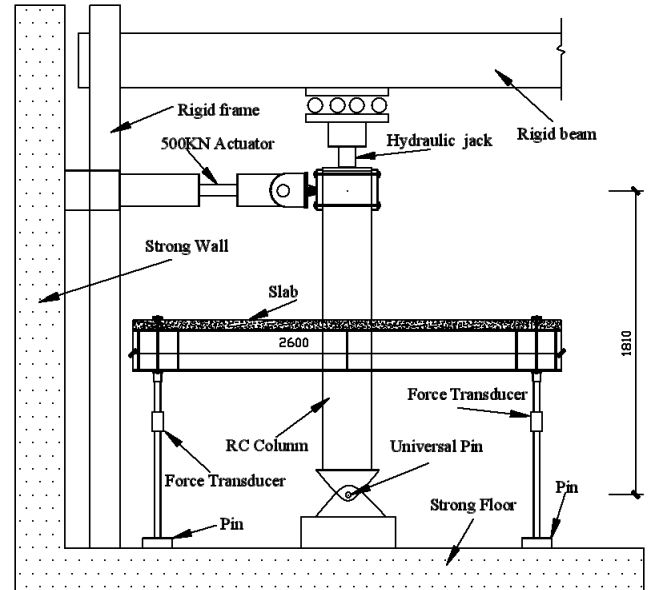


Fig. 4 Test apparatus

3. Test setup, displacement history, and instrumentation

The test setup used for the experimental program is shown in Fig. 4. All columns and beams were pin-connected at their ends to simulated inflection points assumed to locate at midspan of beams and midheight of columns in a laterally loaded frame. The pin at the ends of the beam was supported by two vertical steel links that allowed horizontal displacements but restrained vertical movements. While the pin at the bottom column end restrained both vertical and horizontal displacements, respectively, the pin at the top column end allowed horizontal displacement by a rolling guide support. Lateral reversed-cyclic displacements were applied at the top of the column through a 500 kN hydraulic actuator to simulate lateral loading by pushing and pulling on the framing column. From the previous studies (e.g., Men *et al.* 2015, Cheng and Chen 2005, Huang 2017), the axial load ratio (axial load divided by axial bearing capacity) of RC columns varies from 0.10 to 0.40. A constant column axial load of 723 kN (near 30% of the column's nominal axial capacity) in this paper was applied to the columns through a hydraulic jack. The load and displacement history includes two stage, as shown in Fig. 5. At First, load cycles applied to the specimen increased by 10 kN in each elastic cycle before yielding. Then, displacement cycles were applied to the specimens, with displacement increases by 12 mm after yielding, which was similar to that of Fan *et al.* (2012). Each displacement level cycle was repeated twice to study the stiffness and strength deterioration at that drift level. When the lateral load reduced to about 85% of the peak load, the test was stopped.

A load cell and a displacement transducer were used to monitor the applied lateral load and displacement at the top of the column, respectively. A displacement transducer was also placed near the bottom of the RC column to monitor slip in the test setup. Three displacement transducers and

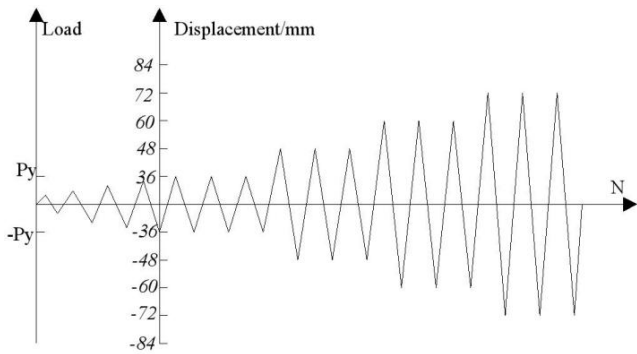


Fig. 5 The loading protocol for specimens

two force transducers were also placed near the two end of the beam to monitor the displacement and vertical load. Linear potentiometers and clinometers were used to measure joint deformations, column and beam rotations. Strains in the steel beam webs and flanges, band plates, cover plates, reinforcement in the column, reinforcement and concrete in the slab, were monitored through linear and rosette strain gauges.

4. Experimental results

4.1 Experimental observation and failure modes

The first of horizontal shear cracking parallel to the continuous beam nearly the top of flange appeared on the surface slab of specimen #1 at approximately 40 kN. Diagonal cracks closed to the column edge and the flexural cracks perpendicular to the continuous beam in the slab started with the increasing of load. Some diagonal cracks that spanned over the full slab width were observed roughly 45 degrees in direction of the horizon axis with an average spacing approximately equal to the depth of the composite beam when the lateral load was 150 kN and the lateral displacement at the top of the RC column was 21 mm. In addition, yielding of the steel beam web near the column faces had started to take place. Column flexural-bearing cracks, which originated from the corners of the band plates located the bottom of column, were also noticed at first displacement level and the slab diagonal cracks became wider; after several displacement cycles, the width of the diagonal cracks near the corner of the RC slab increased to 5 mm; at the same time a quantity of reinforcement in the RC slab gradually yielded. At second displacement level, the flanges of the steel beam started to buckling and the steel beam web appeared oblique texture at a distance near the column faces. Due to the progressive increase in displacement, the cracks propagated and widened gradually. At fourth displacement level, the degree of concrete crushing increased at the end of the column just above and below the band plates. Additionally, the cause of weld cracking in the band plates owed to high compressive stresses within the connection. When the lateral load reduced to about 85% of the peak load, the loading process was terminated. The failure photos of each component of specimen #1 are shown in Fig. 6.

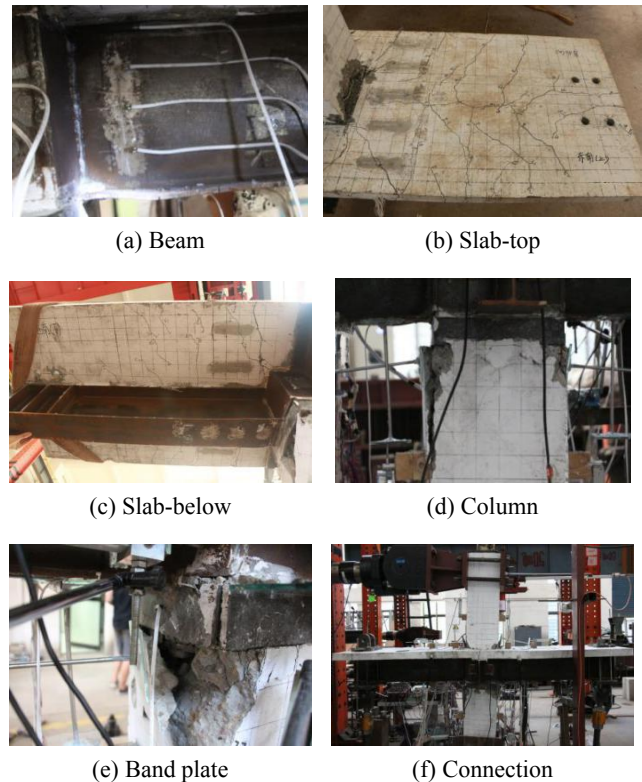


Fig. 6 Failure mode of specimen #1

The test phenomenon and the loading procedure of specimens #2 and #3 were almost the same as those of specimen #1 except for some differences, which would be discussed below. Firstly, the flexural cracks and diagonal cracks became the main features, and the crushed area of concrete in the corner of slab located the bottom of column was gradually enlarging with the increased width of the RC slab. Secondly, the yielding of the steel beam web and buckling of the steel beam flanges delayed had a large load and displacement level. Thirdly, the degree of concrete crushing in the column was weakened and the column remained with only moderate damage at the end of the test.

The steel beam flanges of specimen #4 started to yield when the lateral load reached 60 kN, and local buckling of that significantly at fourth displacement level. The first diagonal crack with a width of 0.10 mm was observed at the east side of the bottom column zone near the band plates at 80 kN and was completely closed after unloading. The steel beams started to yield at first displacement level, and they yielded significantly at third displacement level. When the displacement at the top of the RC column increased to 36 mm, the concrete cover at the west and the south side in column near the joint peeled off. After several cycles, damage accumulated in the concrete of the column zone became more severe. When the displacement at the top of the column increased to 84 mm, the concrete at the bottom column zone crushed and the loading process was terminated. Compared with specimen #4, the concrete in the specimens with the RC slab did not severely spall near the joint in the column due to the increasing constrain of the joint by the involvement of cast-in-situ slab.

The test results displayed that all specimens performed

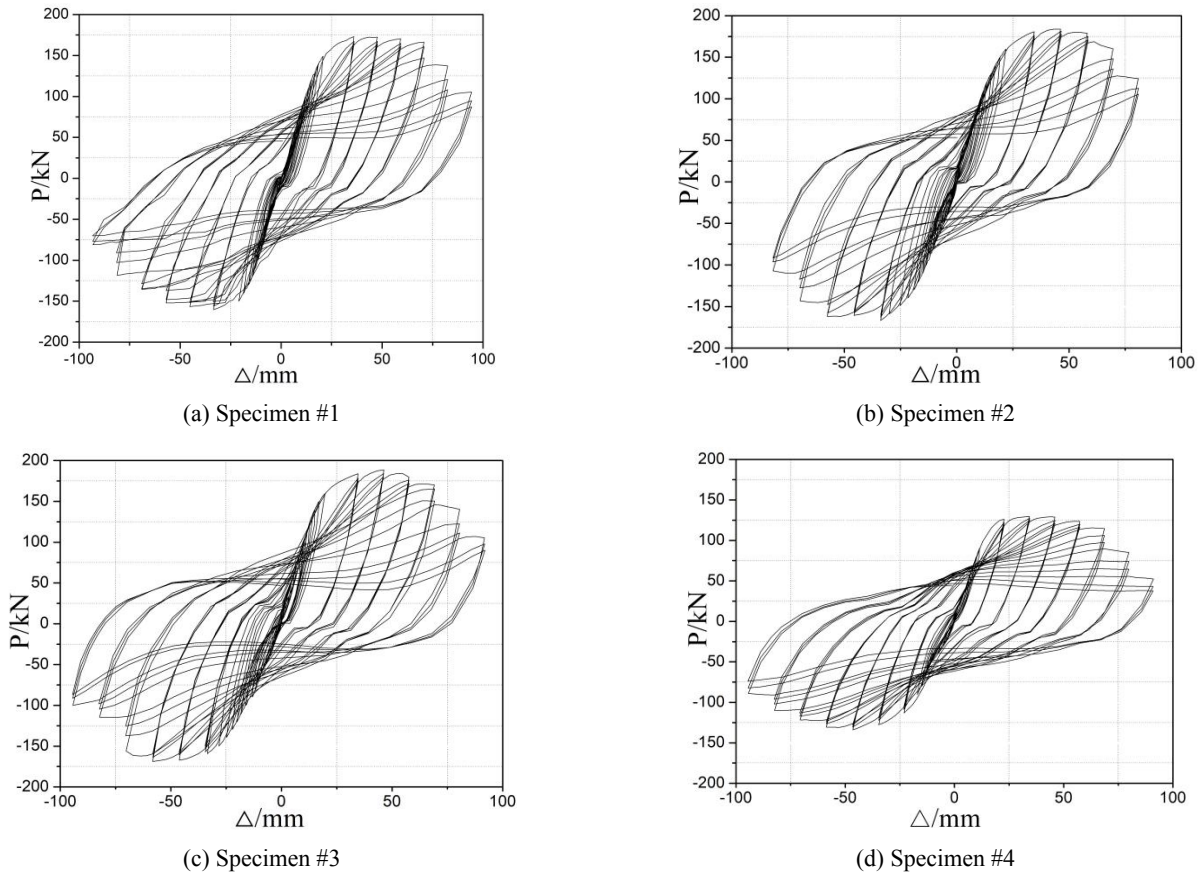


Fig. 7 Hysteretic loops of specimens

in a ductile manner with plastic hinges formed at the beam ends in the vicinity of the column faces, where local buckling took place successively at the beam flange and web, and same damage that included crushed concrete was observed in the column. Visual observation revealed that all specimens except specimen #4 performed similarly, with yielding and local buckling of the beam bottom flange occurring at approximately 100~130 kN and nearly second displacement level, respectively. It should be noted that plastic hinges of the steel beam delayed, due to the increasing moment of beam section by the involvement of cast-in-situ slab under tension led to small beam rotations, was observed during these displacement levels with the increased width of the RC slab. While yielding and local buckling of specimen #4 without the RC slab started at 60 kN and 48 mm. In addition, the test results shown that all specimens followed a strong column-weak beam design philosophy as expected by researchers.

4.2 Load versus displacement response

The specimen behaviour is described by a plot of the horizontal load at upper column against lateral displacement. The reversed cyclic load versus displacement ($P-\Delta$) hysteretic curves of the four specimens are shown in Fig. 7. It can be seen that the hysteretic loops of the three specimens with the RC slab are plump with an inverse “S” shape, and symmetrical in the two loading directions. While that of specimen #4 is nearly a bow shape.

For the specimens with the RC slab, evident pinching can be noticed in the hysteretic loops in the early stage and the subsequent displacement levels, primarily due to some reasons such as the diagonal crackings and the flexural crackings of the RC slab, constrained the rotational capacity of the steel beams by the width of cast-in-situ slab, shear failure of the RC slab near the steel beam flanges leading to relative slip, and some small movement of the supporting frame respecting to the laboratory strong floor especially specimen #1 in pulling direction. However, at larger displacement cycles, during which large beam unelastic deformations occurred, full hysteresis loops that led to good energy dissipation capacity were observed. For specimen #4, there was almost no residual deformation at early loading cycle although some hairline diagonal cracks were observed in the RC column. At larger displacement cycles, the residual deformation was relatively larger on account of the steel beam rotation and the hysteresis loops was full, which resulted in excellent energy dissipation capacity. The features of that maybe attributed to specimen #4 without the RC slab and some damage in the column.

It should be noticed that all the hysteresis loops were stable even at the fourth displacement cycle for the test specimens. The drops in lateral strength after the specimens reached their maximum lateral capacity, as shown in Fig. 7, were mainly caused by local buckling of the steel beam and concrete crushing of the bottom column near the joint. With the increased width of the RC slab for the specimens, the hysteresis loops kept on full and had a strong trend for

deformation capacity. This might be that the RC slab constrained concrete in the joint and enhanced the integrity of the connection. The difference of the hysteretic curves for four specimens indicated that the RC slab had much effect on the seismic behavior of RCS connections. Compared with specimen #4, the load carrying capacity and energy dissipation capacity of the specimens with the RC slab had a better performance. Generally, all specimens with proposed details demonstrated ductile behavior and excellent energy dissipation capacity.

4.3 Enveloped load - displacement curves

An envelope curve can be generated by interconnecting the peak loading points through the reversed cyclic load versus displacement to describe the major seismic characteristics under reversed-cyclic loading. The enveloped load-displacement curves for each of four specimens are shown in Fig. 8, from which the RC slab is proved to be very important to the crack resistance of composite connections and the rotational capacity of the steel beams. Moreover, the bearing capacity can be significantly improved by the RC slab. As shown in Fig. 8,

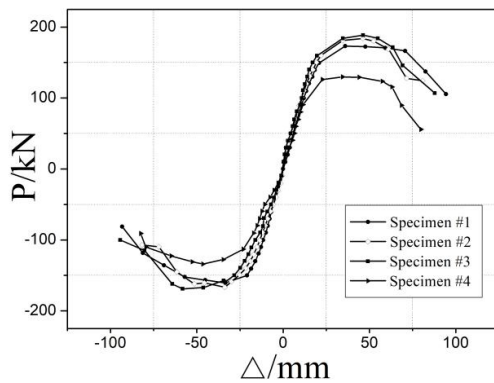


Fig. 8 Comparison of envelope curves

the reversed load-displacement curves of specimens #1, #2 and #3 are almost the same.

4.4 Strength and lateral displacement

On the basis of envelope curves, experimental results on the strength and the displacement are shown in Table 3. P_y , P_{max} and P_u represent the yielding strength, peak strength and the ultimate strength, respectively. Δ_y , Δ_{max} , Δ_u and θ_y , θ_{max} , θ_u are the corresponding displacement and inter-story drift ratio. These parameters are determined from the envelope curve of the hysteresis loops shown in Fig. 8. The ultimate displacement is defined as displacement corresponding to 85% capacity of peak strength. The yield strength and displacement of specimens were determined based on the general yielding method (Tang 1989).

Table 3 shows that the strength of specimens with the RC slab are almost the same, which means the increased width of the RC slab has a little effect on the bearing capacity due to the limitation of effective flange width for composite beam-slab section in a certain structure. The strength of the other two specimens is larger than specimen #1. The orders from high to low are specimens #3, #2 and #1. And compared with specimen #1, the average rate increased in yielding strength, peak strength are approximately 5.7%, 2.0% and 2.2%, 7.2%, respectively. This result is attributed to the increasing moment of beam section and the area of joint constrained by the involvement of the cast-in-situ slab under reversed-cyclic loading. In contrast to specimen #4, the rate increased in average strength of each stage of specimens is about 32.0%, 31.7% and 31.7%, respectively. The strength of specimens with the RC slab have a significant improvement, which means the RC slab makes a remarkable contribution to the bearing capacity of the RCS joints. Table 3 also demonstrates that the average ratio between the maximum force P_{max} and the yielding force P_y for specimens is about 1.16, which indicates that after yielding the strength of the specimen increased about by 16%. This ratio is an important response

Table 3 Test results of specimens

Number	Direction	P_y /kN	Δ_y /mm	θ_y /rad	P_{max} /kN	Δ_{max} /mm	θ_{max} /rad	P_u /kN	Δ_u /mm	θ_u /rad	μ
Specimen #1	+	154.0	23.8	1/77	173.1	36.0	1/51	147.1	74.9	1/24	3.15
	-	-144.2	-24.0	1/76	-160.5	-33.5	1/55	-136.4	-68.5	1/27	2.85
	Average	149.1	23.9	1/76	166.8	34.7	1/53	141.7	71.7	1/25	3.00
Specimen #2	+	141.8	17.7	1/95	183.9	46.2	1/40	156.3	68.1	1/27	3.55
	-	-146.6	-24.2	1/76	-166.7	-33.8	1/54	-141.7	-67.6	1/27	2.79
	Average	144.2	21.0	1/84	175.3	40.0	1/46	149	67.8	1/27	3.17
Specimen #3	+	149.3	17.0	1/108	188.6	46.3	1/40	160.3	72.7	1/25	4.28
	-	-155.6	-31.5	1/58	-168.9	-58.3	1/31	-143.6	-73.6	1/25	2.34
	Average	152.4	24.2	1/75	178.7	52.3	1/35	151.9	73.1	1/25	3.31
Specimen #4	+	105.3	16.2	1/113	129.7	34.4	1/53	110.2	64.2	1/32	3.96
	-	-119.9	-28.5	1/64	-134.0	-46.5	1/39	-113.9	-74.8	1/24	2.62
	Average	112.6	22.3	1/82	131.8	40.4	1/45	112.1	69.5	1/27	3.29

*Note : push (+) and pull (-)

characteristic of the specimen and called specimen load sustainability.

Additionally, the rate increased in yielding displacement and ultimate displacement for specimens is similar to the strength of that as previously mentioned, respectively. The yielding inter-story drift ratio of the specimens ranges from 1/89 to 1/76, which is beyond under seismic loading for the life safety performance level. It is beyond twice to triple times as that of either traditional RC frame or steel structures, which generally are about 1/550 or 1/250. And the ultimate displacement for the specimens is twice times versus conventional steel or concrete special moment frame systems, which generally are about 1/50 given in the Tall Building provisions (CMC 2010b).

4.5 Ductility

The ductility of a structure is evaluated by the quantity of the energy which may be dissipated through plastic deformations. The ductility concept is used in the practice of seismic resistant design and allows, depending on the used structural system, to reduce the seismic forces and to control the level of damages produced especially under seismic excitations.

The displacement ductility of specimen is represented by the displacement ductility coefficient μ which is defined as the ratio of ultimate displacement Δ_u to the yield displacement Δ_y , shown in Table 3. It should be clearly shown that the displacement ductility coefficient of all specimens got in positive direction was more than that of negative direction due to the damage accumulation of concrete. Table 3 also shows that the displacement ductility coefficient of each specimen is larger than 3.0 and the average value of the four specimens is 3.19, which is enough to meet the deformation requirement for earthquake resistant structures, even the RC slab failed earlier than the beam or the column when subjected to severe earthquake loading. Additionally, the displacement ductility coefficient of the specimens with the increased width of the RC slab in table 3 are 3.00, 3.17 and 3.31. Compared with specimen #4, the results show the ductility responses of composite connections are little influenced by the RC slab.

4.6 Strength degradation

The strength degradation is measured by a strength degradation coefficient λ , which is defined as $\lambda_j = Q_{j2,max} / Q_{j1,max}$ where $Q_{j2,max}$ is the peak load of the second cycle at j displacement level, and $Q_{j1,max}$ is peak load of the first cycle at j displacement level. The λ versus Δ curves of the four specimens are shown in Fig. 9.

From Fig. 9, it can be seen that the curve of the strength degradation coefficient of the specimens which vary from 0.7 to 1.0 are relatively smooth. It indicates the cracking of concrete and the yielding of the steel beam are more gentle and complete. Besides, the strength degradation coefficient of specimen #4 is less than that of the others in general before at -48 mm to 48 mm due to lack of the RC slab. Beyond the displacement level of ± 60 mm, the strength degradation coefficient decrease suddenly, which is mainly because concrete crushing under the band plates and the

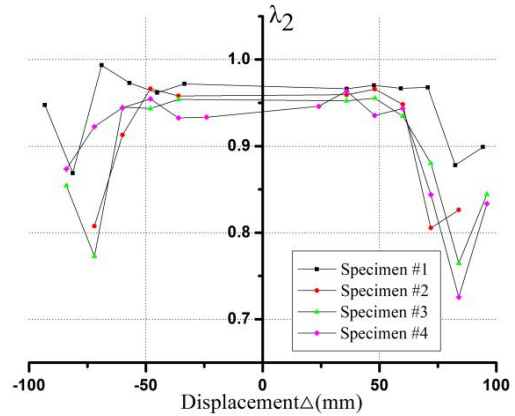


Fig. 9 Strength degradation curves

bulking of the steel beam, respectively. Ultimately, these phenomena indicate that strength degradation can be slowed down and the seismic performance of RCS connections can be improved by proper details and the RC slab.

4.7 Energy dissipation

The energy dissipation characteristics of a structure are commonly used to quantify its seismic performance. Energy dissipation capacity (E_d) at each level is calculated from the enclosed area within the hysteresis loop at this level. The definition of the dissipated energy coefficient is the area of one hysteresis loop divided by the area of the corresponding triangle at each loading cycle obtained the peak positive and negative loads during the first cycle performed at each displacement level. Fig. 10 shows that the energy dissipation of the four specimens are almost the same in the early stage (before 30 cycles) except specimen #4 (between 18 and 30 cycles). However, with the increase of the loading cycle, the energy dissipation curves differ very much. The energy dissipation of the specimens #2 and 3 performed in a similar manner, while that of specimen #1 is larger in the latter level. This indicates that the increased width of slab have a little effect on the energy dissipation capacity of the specimens due to the different crack models of failure for the RC slab.

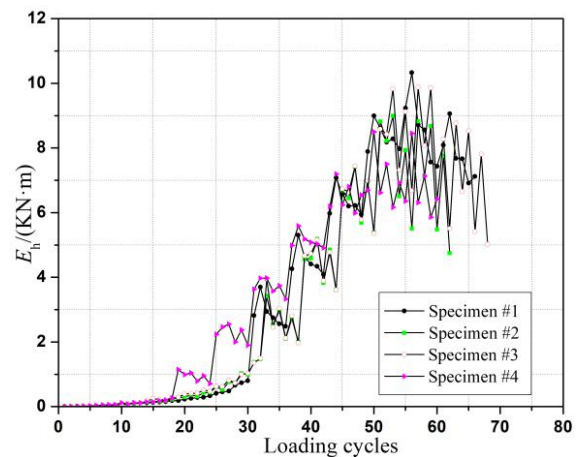


Fig. 10 Energy dissipation curves

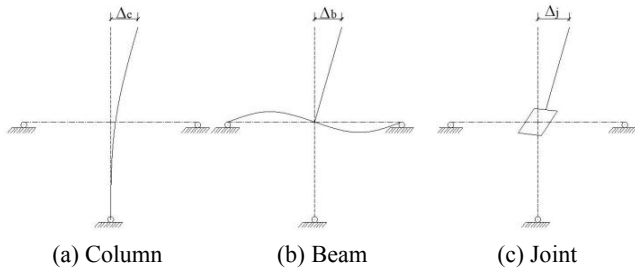


Fig. 11 Column tip deformation analysis sketch

Meanwhile, the equivalent viscous damping coefficient (h_e) obtained by the equation of $E_d/2\pi$ is an another important measure of evaluating the seismic performance of a structure within the hysteresis loop at peak load level. As shown in Table 4, the coefficient of the four specimens are 0.200, 0.199, 0.190 and 0.177, respectively.

Compared with that of RC structure which generally is about 0.1, the equivalent viscous damping coefficient of the specimens is nearly about twice times to indicate that this framing system may represent a viable alternative for low-to-mid-rise structures in high seismic risk zones. It is worth mentioning that the behavior shown in Table 4 for the specimens with the RC slab is representative of the energy ratios exhibited by specimen #4 to manifest that the RC slab may obviously improve the seismic performance of

composite connections.

4.8 Displacement of column

As shown in Fig. 11, studying the contribution of the tip displacement to have a better understood of the behavior of RCS composite specimens, three major mechanisms contributed to the total column tip displacement in the test subassemblies: (a) joint deformations; (b) beam deformations, including elastic and plastic deformations; (c) column deformations, which are calculated, using the following equations

$$\phi_j = (\Delta_2 - \Delta_1) / h_{bf} - (\Delta_3 - \Delta_4) / h_{cf} \quad (1)$$

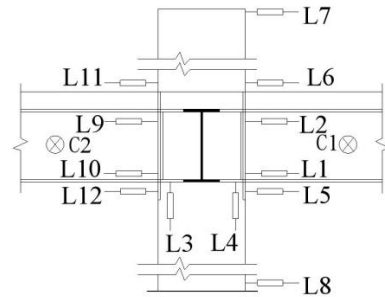
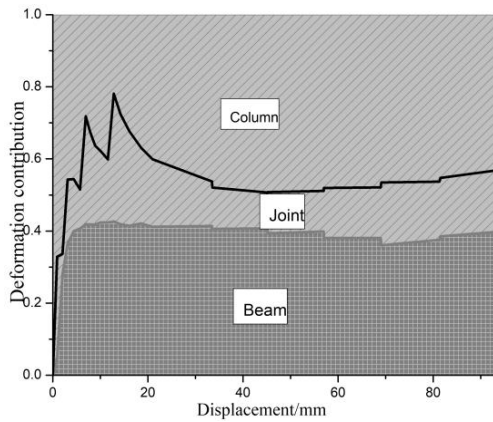
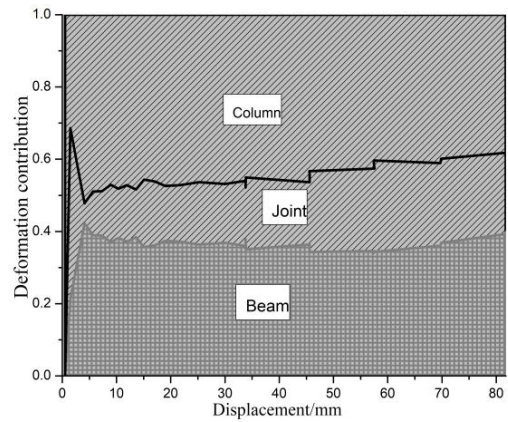


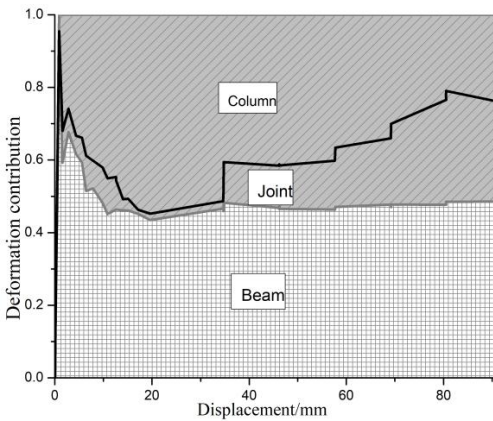
Fig. 12 Deformation measuring methods



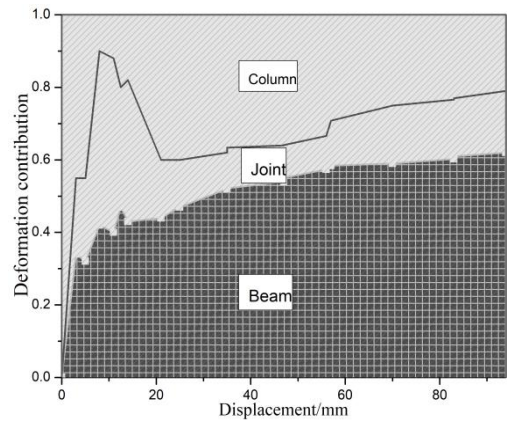
(a) Specimen #1



(b) Specimen #2



(c) Specimen #3



(d) Specimen #4

Fig. 13 Column tip deformation analysis results

$$\delta_j = \phi_j \times h_j \quad (2)$$

where Δ_1 , Δ_2 , Δ_3 and Δ_4 are the displacements recorded from Linear potentiometers, which were attach to right and bottom of joint, h_{bf} was the distance of Δ_1 and Δ_2 , and h_{cf} was the distance of Δ_3 and Δ_4 , respectively. A_j is the joint rotation, h_j is the distance between joint and column tip, and δ_j is the contribution of joint deformation.

$$\delta_b = \phi_b \times h_b \quad (3)$$

$$\delta_c = \delta_t - \delta_j - \delta_b \quad (4)$$

where A_b is the beam rotation recorded from the Linear clinometers, which are attached to web of steel beam, h_b is the distance between steel beam and column tip, and δ_b is the amount of elastic and inelastic deformations of steel beam. δ_c is the contribution of column deformation, and δ_t is the total of column tip displacement. Fig. 12 shows the configuration of the arrangement of Linear potentiometers and clinometers on the test specimens.

The ratios of the distribution of steel beam, column & joint deformations in total displacement are shown in Fig. 13 for the specimens. It is clearly seen that the contribution of joint cores deformation to the overall specimen displacement also decreases due to the coupling effect in the columns and beams with the RC slab and the advantage of slab should be recommended in the design of RCS composite connections.

5. Conclusions

Structural tests on four specimens with or without the RC slab were performed, from which the following conclusions can be drawn:

- An experimental study on the behavior of a novel type of interior RCS beam-column subassemblies following a strong column-weak beam philosophy showed that all specimens performed in a ductile manner with plastic hinges formed in the beam ends near the column faces.
- The specimens revealed a good seismic performance with stable load versus displacement response, high strength, excellent energy dissipation, large beam rotations, and only minor to moderate joint damage.
- The crack resistance and bearing capacity of specimens #2 and #3 are better than specimen #1, which means the width of the RC slab has a significant effect on the behavior of RCS connections. Due to the increasing moment of beam section by the involvement of cast-in-situ slab under reversed-cyclic loading, the specimens provide enhanced ductility and bearing capacity of the composite connections.
- The comparison between the specimens with and without the RC slab indicated that it can obviously improved the seismic performance of the composite connection. The composite effect of the RC slab and

beam should provide references for the seismic analysis of RCS composite frame structure.

- The contribution of joint deformation to the overall specimen displacement also decreases due to the coupling effect in the columns and beams with the RC slab, which should be recommended in the design of RCS composite connections.

Acknowledgments

Funding was provided by the National Key R&D Program of China (Grants 2017YFC0703406). The generous support is gratefully acknowledged. The writers are also grateful to the reviewers for their useful comments and suggestions.

References

- ACI (American Concrete Institute) (2014), Building code requirements for structural concrete (ACI 318-14) and commentary, ACI 318-14, Farmington Hills, MI, USA.
- AISC (2010), Specification for structural steel buildings, American Institute of Steel Construction; Chicago, IL, USA.
- Alizadeh, S., Nader, K.A. and Kazemi, M.T. (2013), "The seismic performance of new detailing for RCS connections", *J. Constr. Steel Res.*, **91**(12), 76-88.
- Alizadeh, S., Attari, N.K.A. and Kazem, M.T. (2015), "Experimental investigation of RCS connections performance using self-consolidated concrete", *J. Constr. Steel Res.*, **114**, 204-216.
- ASCE Task Committee on Design Criteria for Composite Structures in Steel and Concrete (1994), "Guidelines for design of joints between steel beams and reinforced concrete columns", *J. Struct. Eng. ASCE*, **120**(8), 2330-2357.
- Bahman, F.A., Hosein, G. and Nima, T. (2012), "Seismic performance of composite RCS special moment frames", *KSCE J. Civil Eng.*, **17**(2), 450-457.
- Cheng, C.T. and Chen, C.C. (2005), "Seismic behavior of steel beam and reinforced concrete column connections", *J. Constr. Steel Res.*, **61**(5), 587-606.
- CMC (2010a), Code for seismic design of buildings (GB 50011-2010), China Ministry of Construction; Beijing, China.
- CMC (2010b), Technical specification for concrete structures of tall building (JGJ 3-2010), China Ministry of Construction; Beijing, China.
- Deierlein, G. and Noguchi, H. (2004), "Overview of US-Japan research on the seismic design of composite reinforced concrete and steel moment frame structures", *J. Struct. Eng. ASCE*, **130**(2), 361-367.
- El-Tawil, S. and Deierlein, G.G. (2001), "Nonlinear analysis of mixed steel-concrete frames. II: Implementation and verification", *J. Struct. Eng., ASCE*, **127**(6), 656-665.
- Fan, J.H., Zhou, H., Nie, J.G. and Li, Q.W. (2012), "Research on seismic responses of 3D joints with CFT column and composite beam under bi-directional loading", *J. Build. Struct.*, **33**(6), 50-58. [In Chinese]
- Farahmand, A., Ghaffarzadeh, H. and Talebian, N. (2013), "Seismic performance of composite RCS special moment frames", *KSCE J. Civil Eng.*, **17**(2), 450-457.
- Gregoria, K. and Harris, M. (2012), "Exterior RC beam-column joints: New design approach", *Eng. Struct.*, **41**, 307-319.
- Habashizadeh, M.H. (2011), "Effects of isotropic and kinematic hardening on the RCS connection due to cyclic loading", *Int. J. Earth Sci. Eng.*, **04**(06 SPL), 534-537.

- Huang, X.H. (2017), “The study on seismic behavior of the spatial beam-column sub-assemblies in different axial compression ratio of a new type of RCS composite structure”, M.S. Dissertation; Huaqiao University, Quanzhou, China.
- Kim, K. and Noguchi, H. (1998), “A study on the ultimate shear strength of connections with RC columns and steel beams”, *J. Struct. Constr. Eng. Archit. Inst. Japan*, **63**(507), 163-169. [In Japanese]
- Kuramoto, H. and Nishiyama, I. (2004), “Seismic performance and stress transferring mechanism of through-column-type joints for composite reinforced concrete and steel frames”, *J. Struct. Eng. ASCE*, **130**(2), 352-360.
- Li, W., Li, Q.N., Jiang, L. and Jiang, W.S. (2011), “Seismic performance of composite reinforced concrete and steel moment frame structures-state-of-the-art”, *Composites: Part B*, **42**(2), 190-206.
- Liang, X.M. and Parra-Montesinos, G. (2004), “Seismic behavior of reinforced concrete column-steel beam subassemblies and frame systems”, *J. Struct. Eng. ASCE*, **130**(2), 310-319.
- Men, J.J., Guo, Z.F. and Shi, Q.X. (2015), “Experimental research on seismic behavior of novel composite RCS joints”, *Steel Compos. Struct., Int. J.*, **19**(1), 209-221.
- Michael, N.B., Joseph, M.B. and Walter, P.M.J. (2000), “Seismic behavior of composite RCS frame systems”, *J. Struct. Eng. ASCE*, **126**(4), 429-436.
- Moore, W. and Gosain, N. (1985), *Mixed systems: Past practices, recent experience and future direction*, (C. Roeder Ed.), ASCE, New York, NY, USA.
- Nguyen, X.H., Nguyenb, Q.H., Le, D.D. and Mirza, O. (2017), “Experimental study on seismic performance of new RCS connection”, *Structures*, **9**, 53-62
- Nie, X., Yang, Y., Fan, J.S., Mo, Y.L. and Nie, J.G. (2017), “Experimental study on steel jacket-concrete composite connections”, *J. Bridge Eng. ASCE*, **22**(4), 040161381-22.
- Parra-Montesinos, G. and Wight, J.K. (2000), “Seismic response of exterior RC column-to steel beam connections”, *J. Struct. Eng. ASCE*, **126**(10), 1113-1121.
- Parra-Montesinos, G. and Wight, J.K. (2001), “Modeling shear behavior of hybrid RCS beam-column connections”, *J. Struct. Eng. ASCE*, **127**(1), 3-11.
- Sakaguchi, N. (1991), “Shear capacity of beam-column connection between steel beams and reinforced concrete columns”, *J. Struct. Constr. Eng. Archit. Inst. Japan*, **56**(428), 69-78. [In Japanese]
- Sheikh, T.M., Deierlein, G.G., Yura, J.A. and Jirsa, J.O. (1989), “Beam-column moment connections for composite frames: part 1”, *J. Struct. Eng. ASCE*, **115**(11), 2858-2876.
- Shen, H.X. (2007), “Research on static behavior of reinforced concrete column-steel beam (RCS) moment joints”, Ph.D. Dissertation; Xi'an University of Architecture and Technology, Xi'an, China.
- Tang, J.R. (1989), *Seismic Resistance of Joints in Reinforced Concrete Frames*, Southeast University Press, Nanjing, Jiangsu Province, China.
- Viest, I.M., Colaco, J.P., Furlong, R.W., Griffis, L.G., Leon, R.T. and Wyllie, L.A. (1997), *Composite Construction Design for Buildings*, ASCE/McGraw-Hill, New York, NY, USA.
- Wakabayashi, M. (1985), *Recent developments for composite buildings in Japan*, (C. Roeder Ed.), ASCE, New York, NY, USA.